



# Orishchinite, a new terrestrial phosphide, the Ni-dominant analogue of allabogdanite

Sergey N. Britvin<sup>1,2</sup> · Mikhail N. Murashko<sup>1</sup> · Yevgeny Vapnik<sup>3</sup> · Anatoly N. Zaitsev<sup>1</sup> · Vladimir V. Shilovskikh<sup>4</sup> · Maria G. Krzhizhanovskaya<sup>1</sup> · Liudmila A. Gorelova<sup>1</sup> · Oleg S. Vereshchagin<sup>1</sup> · Evgeny A. Vasilev<sup>5</sup> · Natalia S. Vlasenko<sup>4</sup>

Received: 18 April 2022 / Accepted: 15 June 2022

© The Author(s), under exclusive licence to Springer-Verlag GmbH Austria, part of Springer Nature 2022

## Abstract

Orishchinite is a new terrestrial phosphide discovered in pyrometamorphic rocks of the Daba-Siwaqa combustion complex in West Jordan. The mineral occurs as an accessory phase in the fused clinopyroxene-plagioclase rock (paralava) texturally resembling gabbro-dolerite. Orishchinite forms resorbed equant grains up to 0.2 mm outrimmed with 0.1–0.2 thick zones of substituting murashkoite, FeP. Chemical composition (electron microprobe, wt%): Ni 38.49, Fe 22.38, Co 0.47, Mo 18.80, P 19.46, Total 99.60, corresponding to the empirical formula  $(\text{Ni}_{1.04}\text{Fe}_{0.64}\text{Mo}_{0.31}\text{Co}_{0.01})_{\Sigma 2.00}\text{P}$  on the basis of 3 *apfu*. The simplified formula is  $(\text{Ni,Fe,Mo})_2\text{P}$  and the ideal one is  $\text{Ni}_2\text{P}$ . Macroscopically, orishchinite grains have yellowish-white colour with metallic lustre. The mineral is brittle. In reflected light, orishchinite is yellowish-white and non-pleochroic. It is very weakly anisotropic ( $\Delta R_{589} = 1.3\%$ ). Reflectance values for the wavelengths recommended by the Commission on Ore Mineralogy of the International Mineralogical Association are [ $R_{\text{max}}/R_{\text{min}}$  (%),  $\lambda$  (nm)]: 48.1/47.5, 470; 50.6/49.4, 546; 52.1/50.8, 589; 54.4/52.9, 650. The crystal structure was solved and refined to  $R_1 = 0.016$  based on 224 unique observed [ $I \geq 2\sigma(I)$ ] reflections. Orishchinite is orthorhombic, space group *Pnma*,  $a$  5.8020(7),  $b$  3.5933(4),  $c$  6.7558(8) Å,  $V$  140.85(3) Å<sup>3</sup>,  $Z = 4$ ,  $D_x = 7.695$  g cm<sup>-3</sup>. The strongest lines of the powder X-ray diffraction pattern [ $d$ , Å] ( $I$ , %) ( $hkl$ ) are: 2.265(100)(112), 2.201(16)(202), 2.142(55)(211), 2.100(35)(103), 1.909(21)(013), 1.811(19)(113), 1.796(31)(020). Orishchinite is dimorphous with transjordanite (hexagonal  $\text{Ni}_2\text{P}$ ) and can be considered the Ni-dominant analogue of allabogdanite.

**Keywords** Pyrometamorphism · Gabbro-dolerite · Phosphide · Jordan · Crystal structure · Hatrurim formation

Editorial handling: L. Bindi

✉ Sergey N. Britvin  
sergei.britvin@spbu.ru

<sup>1</sup> Institute of Earth Sciences, Saint-Petersburg State University, Universitetskaya Nab. 7/9, 199034 St. Petersburg, Russia

<sup>2</sup> Nanomaterials Research Center, Kola Science Center of Russian Academy of Sciences, Fersman Str. 14, 184209 Apatity, Murmansk Region, Russia

<sup>3</sup> Department of Geological and Environmental Sciences, Ben-Gurion University of the Negev, POB 653, 84105 Beer-Sheva, Israel

<sup>4</sup> Geomodel Resource Center, Saint Petersburg State University, Ulyanovskaya Str. 1, 198504 St. Petersburg, Russia

<sup>5</sup> Saint Petersburg Mining University, 2, 21st Line, 199106 St. Petersburg, Russia

## Introduction

In contrast to arsenides known as the ore-forming minerals in many types of metal deposits (e.g., Berry 1971; Leblanc 1986; Martin-Crespo et al. 2004; Burisch et al. 2017), phosphides are considered exotic minerals on Earth. Since the first reports on schreibersite  $\text{Fe}_3\text{P}$  in native iron from the Disko island in Greenland (e.g., Pauly 1969; Pedersen 1981), several new findings of terrestrial phosphides were described. These occurrences can be subdivided according to their proposed origin. Fe-Ni phosphides are known as phosphate reduction products in fulgurites – natural silicate glasses formed as a result of the lightning strikes (e.g., Essene and Fisher 1986; Pasek et al. 2012; Minyuk et al. 2014; Plyashkevich et al. 2016). Loose Fe-Ni phosphide grains occasionally found in placer deposits likely have cosmogenic (meteoritic) origin (Eremenko et al. 1974; Chen

et al. 1983). Iron phosphides in the assemblages of burned coal dumps (e.g., Nishanbaev et al. 2002), albeit formed as a result of anthropogenic activity, are now treated as minerals (Miyawaki et al. 2019). A separate group of phosphides is comprised by the phases which were not found *in-situ* in rock samples but were detected in heavy mineral concentrates from bulk rock probes subjected to mechanical grinding. This pool of phosphides, along with some other super-reduced phases, was reported from chromite probes originating from three chromium mines: Alapaevsk, Middle Urals, Russia (Zaccarini et al. 2016; Sideridis et al. 2018); Agios Stefanos, Central Greece (Ifandi et al. 2018; Sideridis et al. 2018; Zaccarini et al. 2019a, b; Bindi et al. 2020) and Cr-11 orebody, Luobusa, Tibet, China (Xiong et al. 2020). Note that, besides of a single grain of Ni<sub>5</sub>P phosphide from Alapaevsk, all these phosphides were extracted from chromites subjected to mechanical grinding and heavy mineral separation. At the end, one should point out two single findings of iron phosphides not related to the listed categories. Borodaev et al. (1982) reported nearly pure schreibersite, Fe<sub>3</sub>P, which formed a pseudomorph after submerged wood collected at the deep bottom of the Red Sea. A single grain of Fe<sub>2</sub>P was reported in garnet peridotite from the drill core (Yang et al. 2005).

Phosphide assemblages of combustion pyrometamorphic complexes of the Hatrurim Formation (the Mottled Zone) in the Dead Sea basin, discovered and explored during last decade (Britvin et al. 2015, 2017b), represent a new type of super-reduced phosphorus speciation (Britvin et al. 2021b), where the diversity of discovered terrestrial phosphides exceeds that observed in extraterrestrial rocks (Britvin et al. 2019a, b, 2020a, b, c; 2022a). It should be noted that recently, the phosphide occurrence of similar origin was described at the Khamaryn-Khural-Khiid combustion metamorphic complex in Eastern Mongolia (Savina et al. 2020; Peretyazhko et al. 2021).

In this paper, we provide a description of a novel phosphide, orishchinite, belonging to the quaternary system Fe-Ni-Mo-P. The mineral is named in honour of Stepan Vasil'ovich Orishchin (Степан Васильевич Орищин) (1955–2012), Soviet and Ukrainian crystal chemist, for his valuable contributions to the crystal chemistry of phosphides, arsenides and silicides of transition metals. Stepan Orishchin is an author of more than 40 articles in this field (e.g., Orishchin and Kuz'ma 1982; Orishchin et al. 1998, 2000, 2002). Both the mineral and its name have been approved by the Commission on New Minerals, Nomenclature and Classification (CNMNC) of the International Mineralogical Association (IMA; reference number 2019-039). The holotype specimen of orishchinite is deposited at the Fersman Mineralogical Museum of the Russian

Academy of Sciences, Moscow, Russia, with the registration number 5408/1.

## Geological setting and occurrence

The Hatrurim Formation, or the Mottled Zone in the Southern Levant is the world largest complex of sedimentary strata that experienced combustion metamorphism (Gross 1977; Burg et al. 1992; Vapnik et al. 2007). This term incorporates the processes of high-temperature and low-pressure calcination and fusion of the sediments caused by the burning of organic matter, and can be classified as a subdivision of pyrometamorphism (Grapes 2011). The outcrops of pyrometamorphic rocks in the Middle East are exposed across the area of 150×200 km<sup>2</sup> and can reach 200 m in thickness (Gross 1977; Britvin et al. 2022b). The majority of outcrops are confined to the surroundings of the Dead Sea basin in Israel, Palestinian Authority and Central-West Jordan. However, the northernmost site belonging to the Hatrurim Formation - the Maqarin springs - is situated on the borderline between Jordan and Syria, at the Unity Dam (El Wahdeh Dam) (Martin et al. 2016). The unprecedented, regional scale of combustion processes occurred in the Mottled Zone has raised numerous hypotheses aimed at explanation of their origin. The most popular ones include burning of bituminous shales (e.g., Gross 1977; Geller et al. 2012) or combustion of natural gas (methane) confined to mud volcanoes (Novikov et al. 2013). The discoveries of mineral phases having possible high-pressure origin inspired the formation scenarios that assume some external event as a trigger for the onset of combustion processes (Britvin et al. 2021c, 2022c). The estimations of geological age of the Hatrurim Formation vary within wide range, from 250 ka to 16 Ma (e.g., Kolodny et al. 2014).

Orishchinite was discovered in the paralavas (fusion-affected sedimentary rocks) exposed in the small quarry operated for marble and phosphorites and located in the Jizah District, Amman Governorate, Jordan (Britvin et al. 2015). From the geological viewpoint, the quarry explores pyrometamorphic lithologies of the Daba-Siwaqa complex - the largest rock field belonging to the Hatrurim Formation. The stratigraphic position of this complex in West-Central Jordan was explored in detail in the course of general geological mapping and prospecting for uranium mineralization (Khoury et al. 2014; Abzalov et al. 2015; Alqudah et al. 2015). The paralavas appear as fused patches of green-grey to brown colour encased within less metamorphosed fine-grained chalks and marls (Fig. 1) (see also Abzalov et al. 2015). The rock-forming constituents of paralavas are millimeter-sized euhedral crystals of clinopyroxene of the join diopside-hedenbergite, and anorthite. Texturally, the

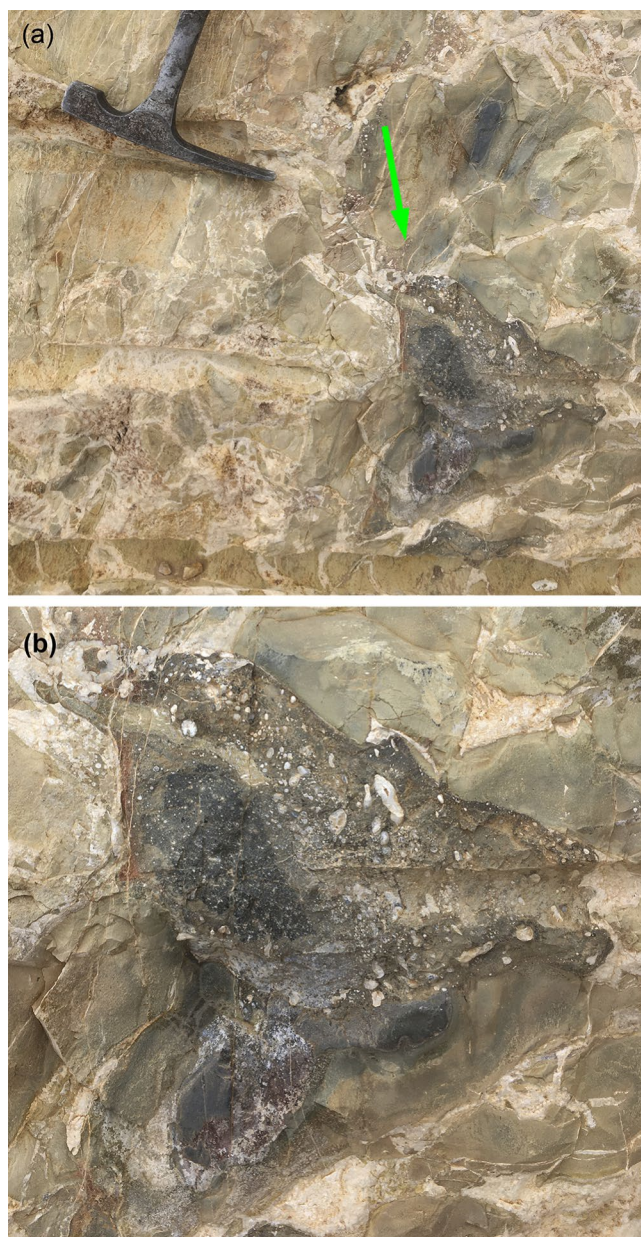


**Fig. 1** Phosphide-bearing paralava (indicated by arrow) in a marble exposed in the wall of the quarry works. (a) General view. (b) Detail showing heterogeneous texture with numerous white voids filled with calcite

paralavas resemble gabbro-dolerites. Accessory minerals are comprised by hematite, pyrrhotite, trevorite, powellite, baryte and another phosphide – nickolayite FeMoP (Murashko et al. 2019). The paralavas contain numerous sub- to millimeter-sized bubbles and voids infilled with late hydrothermal calcite.

## Samples and methods

A 5 cm piece of phosphide-bearing paralava has been cut into a few slices, having an approximate thickness of 5 mm each. The sections have been polished from both sides and were examined in reflected light under polarizing microscope. The areas suspected for the presence of phosphides were marked and, after coating with conductive carbon film, were subjected to electron microprobe investigation. The analyses were carried out in a wavelength-dispersive mode by means of an Oxford Instruments INCA WAVE 500 WDX spectrometer (20 kV, 15 nA) attached to a Hitachi S-3400 N SEM. Pure Ni, Fe, Co metals ( $K\alpha$ -lines), Mo metal ( $L\alpha$ ) and InP ( $PK\alpha$ ) were used as analytical standards. Reflectance values of orishchinite were measured after removal of carbon film, using a Leica DM4500P microscope and Tidas MSP 400 VIS spectrophotometer calibrated against Si standard. Microhardness was not measured to avoid possible damage or loss of brittle orishchinite grain intended for subsequent X-ray single-crystal study. Orishchinite (i.e., Ni-dominant) part of the grain shown in Fig. 2 was hand-picked from the polished section using the tungsten carbide needle, and then used for the X-ray structural investigation. The latter was performed by means of a Bruker Kappa APEX DUO CCD diffractometer using  $MoK\alpha$  radiation. The collected data were processed using a standard built-in set of Bruker programs (Bruker 2004, 2005). The crystal structure was solved and refined using *SHELX*-2015 software incorporated into Olex2 v.1.2 graphical user interface (Sheldrick 2015; Dolomanov et al. 2009). Further details of data collection and structure refinement can be retrieved from the Crystallographic Information File (CIF) included into Supplementary information. The remaining part of composite orishchinite-allabogdanite grain (Fig. 1) was carefully broken into 15–20 grains which were embedded into epoxy resin, polished and checked with electron microprobe. A few more grains cor-

responding to orishchinite were detected, allowing X-ray powder diffraction study conducted with a Rigaku R-AXIS Rapid II diffractometer, curved (cylindrical) imaging plate detector ( $r = 127.4$  mm), using  $CoK\alpha$  radiation ( $\lambda = 1.79021$  Å); rotating anode (40 kV, 15  $\mu$ A) with microfocus optics; Debye-Scherrer geometry, exposure time 60 min. The image plate-to-profile data conversion was performed with *osc2xrd* program (Britvin et al. 2017a). Unit-cell refinement, indexing and calculated pattern were carried out with *STOE WinXPOW* v. 2.08 set of programs (Stoe 2003).

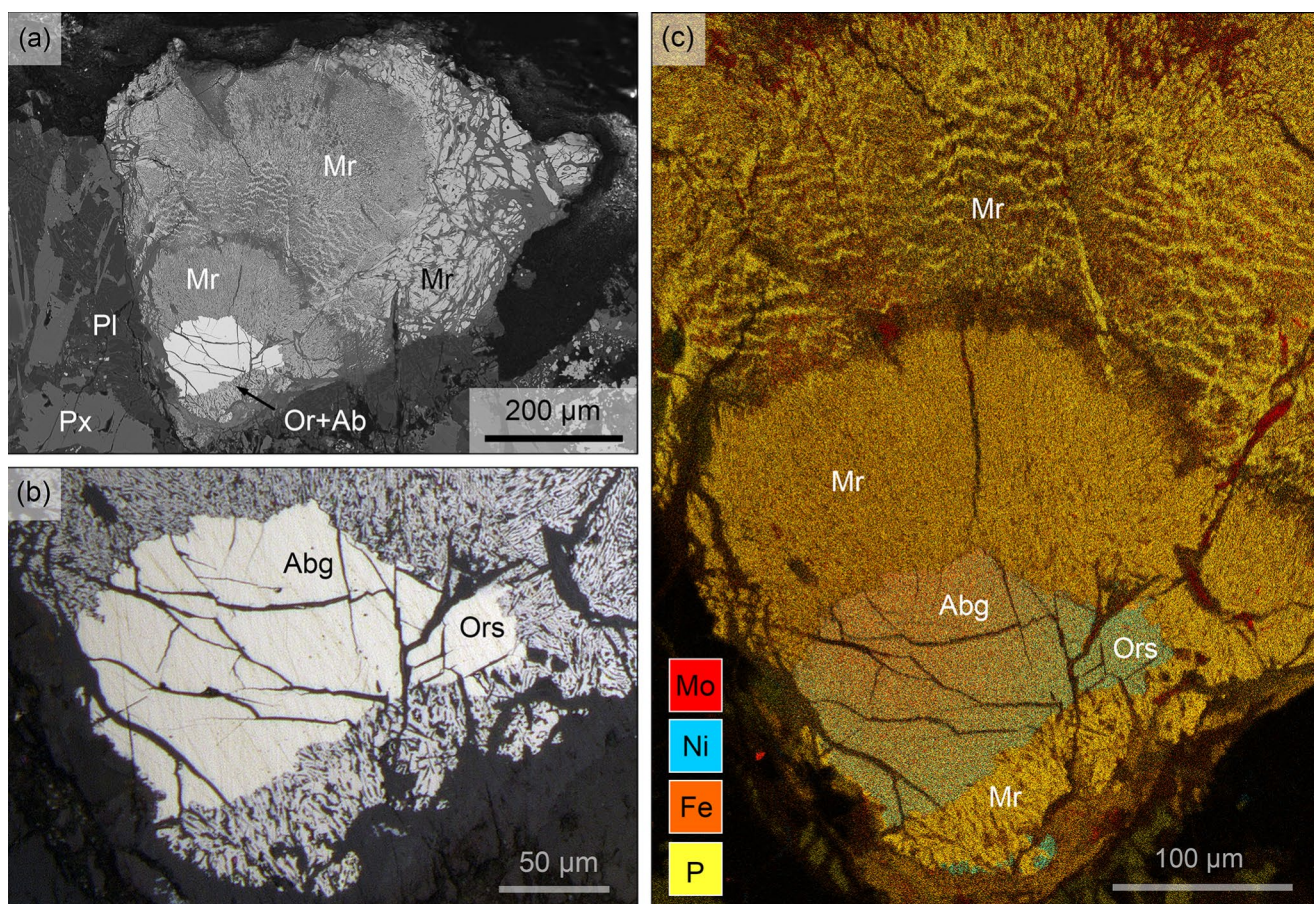


**Fig. 2** (a) General view of orishchinite-bearing phosphide assemblage (Or + Ab) surrounded by a thick zone of murashkoite aggregates in pyroxene-plagioclase parala. SEM BSE image. (b) Detail of a view (a): allabogdanite-orishchinite grain surrounded by an aggregate of vermicular murashkoite. Photo in reflected light. (c) False color EDX elemental map of the same assemblage showing distribution of the main elements (Mo, Ni, Fe, P) across the allabogdanite-orishchinite grain. Orishchinite,  $(\text{Ni,Fe,Mo})_2\text{P}$ , constitutes a small ( $\sim 50 \mu\text{m}$ ) part of a grain which is mapped by blue-green (Ni-dominant) color. Legend: Px, pyroxene; Pl, plagioclase, Mr, murashkoite, FeP; Or, orishchinite; Ab, Mo-rich allabogdanite,  $(\text{Fe,Ni,Mo})_2\text{P}$

## Appearance, chemical composition and physical properties

Orishchinite constitutes a small part of an irregularly shaped Ni-Fe-Mo phosphide grain reaching 0.2 mm in size, which was found in pyroxene-plagioclase matrix of parala (Fig. 2). The grain in whole is comprised by a single crystal of phosphide with the stoichiometry  $M_2\text{P}$  ( $M=\text{Ni, Fe, Mo}$ ) (Fig. 2a,b), whose main part, having Fe-dominant composition, formally belongs to a Ni- and Mo-rich variety of allabogdanite (Britvin et al. 2002, 2021c) (Table 1). The chemical composition of the phosphide gradually changes across the grain, and a small,  $\sim 50 \mu\text{m}$  area at the grain corner is represented by orishchinite (Fig. 2a,b; Table 1). The whole orishchinite-allabogdanite grain is corroded and surrounded by a “corona” up to 0.5 mm in width, composed by three zones of murashkoite, FeP (Britvin et al. 2019b) (Fig. 2; Table 1). The appearance and texture of murashkoite

corona is the same as in the previously described intergrowths with barringerite, transjordanite and allabogdanite (Britvin et al. 2019b, 2020a, 2021c).

Murashkoite zones adjacent to orishchinite-allabogdanite interface appear as aggregate of vermicular microcrystals, whereas the outer rim is composed of coarse-granular murashkoite. In reflected light, orishchinite and allabogdanite parts belonging to the same grain are indistinguishable; they have the same yellowish-white colour, with no observable birefractance or anisotropy. Reflectance values for orishchinite are provided in Table 2. The mineral is very brittle. The estimated Mohs’ hardness is between 5 and 6. The density calculated from the unit-cell parameters (single-crystal data) and empirical formula (Table 1) is  $7.500 \text{ g cm}^{-3}$ . Chemical composition of orishchinite corresponds to a simplified formula  $(\text{Ni,Fe,Mo})_2\text{P}$  with  $\text{Ni} > \text{Fe} > \text{Mo}$ ; allabogdanite,  $(\text{Fe,Ni,Mo})_2\text{P}$  has Fe-dominant composition (Table 2). The orishchinite-allabogdanite grain contains

**Table 1** Chemical compositions and calculated formulae of orishchinite, coexisting allabogdanite and murashkoite

Constituent	Orishchinite		Allabogdanite		Murashkoite	
	(n = 7) Mean	min; max; esd	(n = 13) Mean (wt	min; max; esd	(n = 5) mean	min; max; esd
Fe	22.38	20.76; 23.66; 0.92	27.42	25.77; 28.69; 0.75	59.33	58.83; 59.95; 0.50
Co	0.47	0.43; 0.51; 0.03	0.44	0.33; 0.53; 0.07	b.d.l.	
Ni	38.49	36.66; 40.53; 1.20	26.32	21.91; 29.33; 2.61	3.99	3.75; 4.45; 0.28
Mo	18.80	18.19; 19.88; 0.53	27.16	24.25; 31.2; 2.66	b.d.l.	
P	19.46	19.40; 19.61; 0.07	18.84	18.32; 19.56; 0.36	36.22	36.03; 36.46; 0.17
Total	99.60		100.18		99.54	
Calculated empirical formula*	$(\text{Ni}_{1.04}\text{Fe}_{0.64}\text{Mo}_{0.31}\text{Co}_{0.01})_{2.00}\text{P}_{1.00}$		$(\text{Fe}_{0.80}\text{Ni}_{0.73}\text{Mo}_{0.46}\text{Co}_{0.01})_{2.00}\text{P}_{0.99}$		$(\text{Fe}_{0.92}\text{Ni}_{0.06})_{0.98}\text{P}_{1.02}$	

All values are quoted in wt%

n = number of analyses

min; max; esd = minimum value; maximum value; estimated standard deviation

bdl = below the detection limite (< 0.05 wt%)

\* Formulae were calculated based on 3 (orishchinite, allabogdanite) and 2 (murashkoite) oxygen atoms per formula unit, respectively

**Table 2** Reflectance values for orishchinite

$R_{\text{max}}$ (%)	$R_{\text{min}}$ (%)	$\lambda$ (nm)	$R_{\text{max}}$ (%)	$R_{\text{min}}$ (%)	$\lambda$ (nm)
45.5	45.2	420	52.5	51.2	600
46.3	46.0	440	53.4	51.8	620
47.4	47.2	460	54.1	52.5	640
<b>48.1</b>	<b>47.5</b>	<b>470</b>	<b>54.4</b>	<b>52.9</b>	<b>650</b>
48.5	47.8	480	54.8	53.3	660
48.8	48.4	500	55.7	54.0	680
49.6	48.7	520	56.4	55.0	700
50.3	49.2	540	56.8	55.8	720
<b>50.6</b>	<b>49.4</b>	<b>546</b>	57.0	56.7	740
51.1	49.9	560	58.9	56.9	760
51.8	50.5	580	59.1	57.8	780
<b>52.1</b>	<b>50.8</b>	<b>589</b>	61.9	58.5	800

Note: Data for wavelengths recommended by the IMA Commission on Ore Mineralogy (COM) are marked in bold font

noticeable contents of Co. In contrast, surrounding murashkoite is devoid of Co and has very low Ni contents (Table 2).

## Crystal structure and powder diffraction

Orishchinite crystallizes in the TiNiSi subtype of  $\text{Co}_2\text{Si}$  structure type, known for extraordinary tolerance towards incorporation of transition metals (Rundqvist and Nawapong 1966; Guérin et al. 1975; Guérin and Sergent 1977), which motivates why  $\text{Co}_2\text{Si}$ -type phosphides are the most numerous among phosphide minerals (Table 3). Orishchinite is the first Ni-dominant mineral in this family. The good quality of X-ray single-crystal data (Table 4) allowed precise refinement of site populations, even the determination of Fe/Ni distribution sharing the same metal sites, as it was recently shown on the schreibersite-nickelphosphide series,  $\text{Fe}_3\text{P}$ - $\text{Ni}_3\text{P}$  (Britvin et al. 2021a). The crystal structure of

orishchinite represents a framework built up of two types of metal-phosphorus polyhedra, tetrahedra [ $M1\text{P}_4$ ] and square-pyramidal [ $M2\text{P}_5$ ] (Tables 4 and 5; Fig. 3). Due to the significant difference in scattering factors of Mo ( $Z=42$ ), and Fe or Ni ( $Z=26$  and 28, respectively), it was not a problem to determine that Mo is incorporated entirely into the  $M2$  position (Table 4). The free refinement of  $M1$  and P sites using scattering curves for neutral Ni and P atoms (Wilson 1992) gave site scattering factors equal to  $28.00 e^-$  for the  $M1$  and  $15.00 e^-$  for the P site, corresponding to site populations of  $\text{Ni}_{1.00}$  and  $\text{P}_{1.00}$ , respectively. These s.o.f. were fixed during the final refinements. The population at the  $M2$  site was freely refined using scattering curves for neutral Fe and Mo atoms, and resulted in the site scattering factor equal to  $33.04 e^-$  that corresponds to the calculated  $M2$  site population of  $(\text{Fe}_{0.56}\text{Mo}_{0.44})$ . These site populations corroborate with the shorter Ni-P bond lengths in tetrahedron [ $\text{NiP}_4$ ] as compared to the longer bonds in square pyramid [ $(\text{Fe},\text{Mo})\text{P}_5$ ] (Table 6). The structural formula of orishchinite is  $\text{Ni}_{1.00}(\text{Fe}_{0.56}\text{Mo}_{0.44})_{1.00}\text{P}_{1.00}$ . However, taking into account wide deviations from the stoichiometry known in  $\text{Co}_2\text{Si}$ -type phosphides (Guérin et al. 1975; Guérin and Sergent 1977; Oliynyk et al. 2013), one can not exclude the possibility of partial substitution of Ni for (Mo + Fe) at the  $M1$  site, and vice versa. The latter can explain the observed discrepancy between the structural and empirical formulae of the mineral. The ideal structural formula of orishchinite could be expressed as  $\text{Ni}(\text{Fe},\text{Mo})\text{P}$ . However, taking into account the pertaining uncertainties in real site populations, and the lack of any reference data on the bond length correlations in these compounds, the formula of orishchinite approved by IMA-CNMNC is  $(\text{Ni},\text{Fe},\text{Mo})_2\text{P}$ . The ideal end-member formula for the mineral is thus  $\text{Ni}_2\text{P}$ , and therefore, orishchinite is currently regarded as the Ni-dominant analogue of allabogdanite, an orthorhombic modification of

**Table 3** Comparison of crystallographic data of orishchinite with that of related phosphide minerals

Mineral <sup>a</sup>	Ideal formula	Structure type	Space group	<i>a</i> (Å)	<i>b</i> (Å)	<i>c</i> (Å)	<i>V</i> (Å <sup>3</sup> )	<i>Z</i>
Orishchinite [1]	Ni <sub>2</sub> P	TiNiSi	<i>Pnma</i>	5.802	3.593	6.756	140.8	4
Allabogdanite [2]	Fe <sub>2</sub> P	Co <sub>2</sub> Si	<i>Pnma</i>	5.792	3.564	6.691	138.1	4
Transjordanite [3]	Ni <sub>2</sub> P	Fe <sub>2</sub> P	<i>P62m</i>	5.884		3.349	100.4	3
Barringerite [4]	Fe <sub>2</sub> P	Fe <sub>2</sub> P	<i>P62m</i>	5.867		3.465	103.3	3
Monipite [5] <sup>b</sup>	MoNiP	Fe <sub>2</sub> P	<i>P62m</i>	5.861		3.704	110.2	3
Florenskyite [6] <sup>b</sup>	FeTiP	TiNiSi	<i>Pnma</i>	6.007	3.602	6.897	149.2	4
Andreyivanovite [7] <sup>b</sup>	FeCrP	TiNiSi	<i>Pnma</i>	5.833	3.569	6.658	138.6	4
Nickolayite [8]	FeMoP	TiNiSi	<i>Pnma</i>	5.952	3.707	6.847	151.1	4
Grammatikopouosite [9]	NiVP	Co <sub>2</sub> Si	<i>Pnma</i>	5.889	3.572	6.815	143.4	4

<sup>a</sup> References: [1] this work; [2] Britvin et al. (2002); [3] Britvin et al. (2015); [4] Buseck (1969); Britvin et al. (2017b); [5] Ma et al. (2014), Guérin and Sergent (1977); [6] Ivanov et al. (2000), Rundqvist and Nawapong (1966); [7] Zolensky et al. (2008), Kumar et al. (2004); [8] Murashko et al. (2019). [9] Bindi et al. (2020)

<sup>b</sup> Crystal structures for natural monipite, florenskyite and andreyivanovite were not determined. The unit cell parameters for monipite have been assigned on the basis of EBSD pattern which matches those of synthetic analogues. The unit-cell parameters for florenskyite and andreyivanovite were determined using synchrotron-based Laue method

**Table 4** Crystal parameters, data collection and structure refinement details for orishchinite

Crystal Data	
Formula *	Ni(Fe <sub>0.56</sub> Mo <sub>0.44</sub> )P
Crystal size (mm)	0.03 · 0.03 · 0.03
Crystal system	Orthorhombic
Space group	<i>Pnma</i>
<i>a</i> (Å)	5.8020 (7)
<i>b</i> (Å)	3.5933 (4)
<i>c</i> (Å)	6.7558 (8)
<i>V</i> (Å <sup>3</sup> )	140.85 (3)
<i>Z</i>	4
<i>D<sub>x</sub></i> (g cm <sup>-3</sup> )	7.695
Data collection and refinement	
Radiation	MoKα (λ = 0.71073 Å)
Temperature (K)	293
2θ <sub>max</sub> (°)	truncated at 60.00
Total reflections collected	1194
No. unique reflections	236
No. unique observed, <i>I</i> ≥ 2σ( <i>I</i> )	224
<i>h</i> , <i>k</i> , <i>l</i> range	−8 → 4, −5 → 4, −9 → 8
<i>F</i> (000)	304
μ (mm <sup>-1</sup> )	23.44
<i>R</i> <sub>int</sub> , <i>R</i> <sub>σ</sub>	0.022, 0.017
<i>R</i> <sub>1</sub> [ <i>F</i> ≥ 4σ( <i>F</i> )], <i>wR</i> <sub>2</sub>	0.016, 0.036
<i>S</i> = <i>GoF</i>	1.14
Residuals (e Å <sup>-3</sup> ) (min, max)	−0.68, 0.60
Data completeness	1.000

\* As determined by site occupancy refinement

Fe<sub>2</sub>P (Britvin et al. 2002). The intensities and indexing of X-ray powder diffraction data for orishchinite (Table 7) confirm the results of X-ray structural analysis.

**Table 5** Sites, Wyckoff positions, fractional atomic coordinates, isotropic displacement parameters (Å<sup>2</sup>) and site occupancies for orishchinite

Site	<i>x</i>	<i>y</i>	<i>z</i>	<i>U</i> <sub>iso</sub>	Occupancy
M1 (4c)	0.64106(9)	3/4	0.43655(7)	0.00690(18)	Ni <sub>1.00</sub>
M2 (4c)	0.02995(8)	3/4	0.66966(6)	0.00665(17)	Fe <sub>0.56</sub> Mo <sub>0.44</sub>
P (4c)	0.25768(17)	3/4	0.37710(14)	0.0049(2)	P <sub>1.00</sub>

## Discussion

The sources of Mo and Ni enrichment in the area of the Dead Sea Transform fault, and the fate of these elements in pyrometamorphic processes have been reviewed in the previous papers (Issar et al. 1969; Gilat 1994; Bogoch et al. 1999; Fleurance et al. 2013; Britvin et al. 2022b). In this article, we focus on the crystal-chemical aspects of Mo-phosphides formation, in particular, on the role of Mo in stabilization of low- or high-pressure phosphides in the polycomponent system Fe<sub>2</sub>P–Ni<sub>2</sub>P–(Mo<sub>2</sub>P). This is a continuation of the discussion on metastable phases having possible high-pressure origin, which were recently discovered in the rocks of the Hatrurim Formation on the Israel side of the Dead Sea basin (Britvin et al. 2021c, 2022c). Although pure Mo<sub>2</sub>P is not known, Mo is readily incorporated into the solid solutions Fe<sub>2</sub>P–Ni<sub>2</sub>P (Guérin et al. 1975; Guérin and Sergent 1977; Oliynyk et al. 2013). In this respect, it has to be noted that phosphides along the tie-line Fe<sub>2</sub>P–Ni<sub>2</sub>P may crystallize in two structural types. The crystal structure of low-pressure, hexagonal Fe<sub>2</sub>P polymorph barringerite (hereinafter LP-Fe<sub>2</sub>P) is characteristic of all (Fe<sub>1-x</sub>Ni<sub>x</sub>)<sub>2</sub>P phosphides formed at atmospheric pressure (Buseck 1969; Britvin et al. 2020a). However, at a pressure beyond 8 GPa, pure LP-Fe<sub>2</sub>P becomes metastable and transforms into a high-pressure, orthorhombic modification (HP-Fe<sub>2</sub>P) (Dera

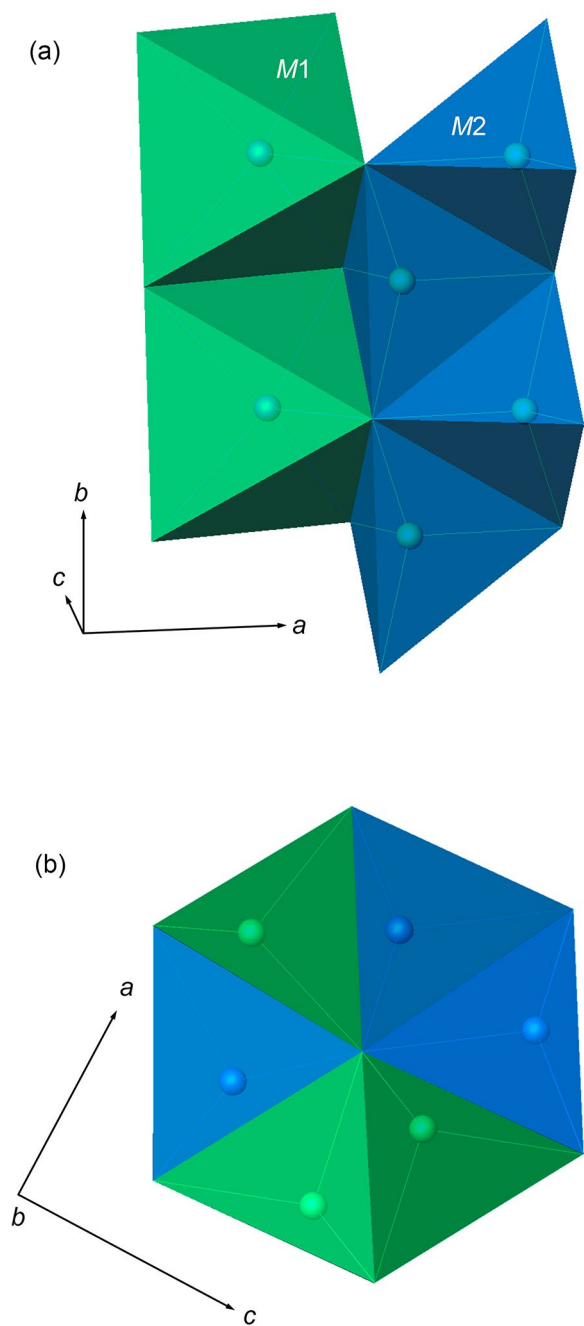


**Fig. 3** Crystal structure of orishchinite. (a) A view slightly inclined relative to the b-axis. Chains (rods) of edge- and corner-sharing square pyramids  $[M1P_5]$  (green) and tetrahedra  $[M2P_4]$  (blue). (b) Projection onto (010) plane

et al. 2008), which crystallizes with the  $Co_2Si$  structure type and is known in nature as the mineral allabogdanite (Britvin et al. 2002, 2019c). A recent work (Litasov et al. 2020) showed that allabogdanite could be synthesized at atmospheric pressure, but these data should be treated carefully as the Raman spectra of obtained phosphide do not

**Table 6** Selected bond lengths (Å) in the crystal structure of orishchinite

Bond	Length	Bond	Length
M1–P	2.2244(11)	P–M1	2.2244(11)
M1–P	2.2604(11)	P–M1	2.2604(11)
M1–P	2.2711(7) × 2	P–M1	2.2711(7)
M2–P	2.3774(11)	P–M2	2.3774(11)
M2–P	2.4724(8) × 2	P–M2	2.4724(8)
M2–P	2.5904(8) × 2	P–M2	2.5904(8)

correspond to the spectra of structurally confirmed allabogdanite (Vereshchagin et al. 2021).

In contrast to  $Fe_2P$ , the high-pressure,  $Co_2Si$ -type modification of  $Ni_2P$  is unknown, and this phosphide persists as a low-pressure, hexagonal form up to 50 GPa (Dera et al. 2009). Consequently, incorporation of Ni into the solid solutions  $(Fe_{1-x}Ni_x)_2P$  would have stabilized the low-pressure, hexagonal modification of these phosphides, displacing the expected onset of the LP-HP transition in the field of pressures exceeding 8 GPa.

Studies in the system  $Fe_2P$ – $Mo_2P$  at atmospheric pressure showed the existence of orthorhombic,  $Co_2Si$ -type  $(Mo_{1-x}Fe_x)_2P$  solid solutions in a very wide compositional range ( $x=0.30$ – $0.82$ ). The hexagonal phase in this range is unknown (Oliynyk et al. 2013). The mineral nickolayite, ideally  $FeMoP$ , discovered in the same rock sample as orishchinite, also crystallizes with the  $Co_2Si$  structure type (Murashko et al. 2019). Consequently, one can conclude that substitution of Fe for Mo in  $(Mo_{1-x}Fe_x)_2P$  phosphides at atmospheric pressure favors stabilization of the  $Co_2Si$  (HP- $Fe_2P$ ) structure type. On the contrary, solid solutions of the join  $Ni_2P$ – $Mo_2P$ , both synthetic and natural ones (the mineral monipite,  $MoNiP$ ) adopt the hexagonal LP- $Fe_2P$  structure type only (Guérin et al. 1975; Guérin and Sergent 1977).

Therefore, the simultaneous incorporation of Mo and Ni into the  $Fe_2P$ -based solid solutions implies superposition of two counter-directional tendencies: stabilization of orthorhombic ( $Co_2Si$ -type) structure by Mo vs. Ni-induced stabilization of hexagonal (LP- $Fe_2P$ ) structure. It has been shown that even subordinate incorporation of Mo and Ni might considerably displace the low- to high-pressure transition boundary, from 8 GPa for pure  $Fe_2P$  to 25 GPa for allabogdanite containing 4 wt% Ni and 2.5 wt% Mo (Britvin et al. 2021c). In case of Ni-dominant and Mo-rich orishchinite,  $(Ni,Fe,Mo)_2P$ , the substitution effect on low- to high-pressure transition boundary might be even stronger, but the latter requires further investigations.

**Table 7** X-ray powder diffraction data ( $d$  in Å) for orishchinite \*

$I_{\text{meas}}$	$d_{\text{meas}}$	$I_{\text{calc}}$	$d_{\text{calc}}$	$hkl$	$I_{\text{meas}}$	$d_{\text{meas}}$	$I_{\text{calc}}$	$d_{\text{calc}}$	$hkl$
8	3.178	3.172	6	011	3	1.479	1.478	2	114
8	2.913	2.919	4	102	3	1.468	1.467	3	303
		2.902	4	200			1.451	1	400
10	2.781	2.784	6	111	2	1.419	1.419	3	401
100	2.265	2.266	100	112	3	1.392	1.392	5	222
		2.258	44	210	15	1.365	1.365	18	123
16	2.201	2.201	12	202			1.359	2	313
55	2.142	2.141	73	211			1.345	1	410
35	2.100	2.099	35	103	3	1.333	1.333	5	402
21	1.909	1.908	24	013	6	1.317	1.320	5	411
5	1.876	1.877	5	212			1.316	4	105
15	1.860	1.860	23	301	8	1.292	1.292	14	321
19	1.811	1.813	15	113	10	1.265	1.265	9	015
31	1.796	1.797	39	020			1.264	6	223
9	1.780	1.779	9	203	1	1.251	1.250	4	412
8	1.688	1.689	5	004	4	1.231	1.231	4	024
13	1.679	1.679	16	302	14	1.226	1.227	12	322
6	1.651	1.652	3	311	7	1.225	1.225	5	205
3	1.622	1.622	2	104	6	1.204	1.204	2	124
5	1.594	1.594	3	213	14	1.199	1.199	21	314
3	1.530	1.530	1	122					
		1.528	1	220					

\* Calculated lines with the intensity less than 1 have been omitted

**Supplementary Information** The online version contains supplementary material available at <https://doi.org/10.1007/s00710-022-00787-x>.

**Acknowledgements** The instrumental and computational facilities for the study were provided by the Scientific Park of Saint-Petersburg State University: Centre for X-ray diffraction studies; Geomodel; Centre for Diagnostics of Functional Materials; Resource Center of Nanotechnology. The authors are thankful to Federica Zaccarini and an anonymous referee for careful examination and discussion of manuscript contents, that substantially improved the final article version. This research was carried out under financial support of the Russian Science Foundation, grant 18-17-00079.

## References

- Abzalov MZ, van der Heyden A, Saymeh A, Abuqudaira M (2015) Geology and metallogeny of Jordanian uranium deposits. *Appl Earth Sci* 124:63–77
- Alqudah M, Hussein MA, Boorn S, van den, Podlaha OG, Mutterlose J (2015) Biostratigraphy and depositional setting of Maastrichtian–Eocene oil shales from Jordan. *Mar Petrol Geol* 60:87–104
- Berry LG (1971) The silver-arsenide deposits of the Cobalt-Gowganda region, Ontario. *Can Mineral* 11:1–429
- Bindi L, Zaccarini F, Ifandi E, Tsikouras B, Stanley C, Garuti G, Mauro D (2020) Grammatikopoulosite, NiVP, a New Phosphide from the Chromitite of the Othrys Ophiolite. *Greece Minerals* 10:131
- Bogoch R, Gilat A, Yoffe O, Ehrlich S (1999) Rare earth trace element distributions in the Mottled Zone complex, Israel. *Isr J Earth Sci* 48:225–234
- Borodaev YuS, Bogdanov YuA, Vyal'sov LN (1982) New nickel-free variety of schreibersite Fe<sub>3</sub>P. *Zap Vsesoyuzn Mineral Obsch* 111(6):682–687 (in Russian)
- Britvin SN, Rudashevsky NS, Krivovichev SV, Burns PC, Polekhovskiy YuS (2002) Allabogdanite, (Fe,Ni)<sub>2</sub>P, a new mineral from the Onello meteorite: the occurrence and crystal structure. *Am Mineral* 87:1245–1249
- Britvin SN, Murasko MN, Vapnik Ye P, Krivovichev YuS SV (2015) Earth's phosphides in Levant and insights into the source of Archean prebiotic phosphorus. *Sci Rep* 5:8355
- Britvin SN, Dolivo-Dobrovolsky DV, Krzhizhanovskaya MG (2017a) Software for processing the X-ray powder diffraction data obtained from the curved image plate detector of Rigaku RAXIS Rapid II diffractometer. *Zap Ross Mineral Obshch* 146:104–107 (in Russian)
- Britvin SN, Murashko MN, Vapnik E, Polekhovskiy YuS, Krivovichev SV (2017b) Barringerite Fe<sub>2</sub>P from pyrometamorphic rocks of the Hatrurim Formation, Israel. *Geol Ore Depos* 59:619–625
- Britvin SN, Murashko MN, Vapnik Ye, Polekhovskiy YuS, Krivovichev SV, Vereshchagin OS, Vlasenko NS, Shilovskikh VV, Zaitsev AN (2019a) Zuktamrurite, FeP<sub>2</sub>, a new mineral, the phosphide analogue of löllingite, FeAs<sub>2</sub>. *Phys Chem Miner* 46:361–369
- Britvin SN, Vapnik Ye, Polekhovskiy YuS, Krivovichev SV, Krzhizhanovskaya MG, Gorelova LA, Vereshchagin OS, Shilovskikh VV, Zaitsev AN (2019b) Murashkoite, FeP, a new terrestrial phosphide from pyrometamorphic rocks of the Hatrurim Formation, Southern Levant. *Mineral Petrol* 113:237–248
- Britvin SN, Shilovskikh VV, Pagano R, Vlasenko NS, Zaitsev AN, Krzhizhanovskaya MG, Lozhkin MS, Zolotarev AA, Gurchiy VV (2019c) Allabogdanite, the high-pressure polymorph of (Fe,Ni)<sub>2</sub>P, a stishovite-grade indicator of impact processes in the Fe–Ni–P system. *Sci Rep* 9:1047
- Britvin SN, Murashko MN, Vapnik Ye, Polekhovskiy YuS, Krivovichev SV, Krzhizhanovskaya MG, Vereshchagin OS, Shilovskikh VV, Vlasenko NS (2020a) Transjordanite, Ni<sub>2</sub>P, a new terrestrial and meteoritic phosphide, and natural solid solutions barringerite–transjordanite (hexagonal Fe<sub>2</sub>P–Ni<sub>2</sub>P). *Am Mineral* 105:428–436
- Britvin SN, Murashko MN, Vapnik Ye, Polekhovskiy YuS, Krivovichev SV, Vereshchagin OS, Shilovskikh VV, Vlasenko NS,

- Krzhizhanovskaya MG (2020b) Halamishite,  $\text{Ni}_5\text{P}_4$ , a new terrestrial phosphide in the Ni–P system. *Phys Chem Miner* 2020:3
- Britvin SN, Murashko MN, Vapnik Ye P, Krivovichev YuS, Vereshchagin SV, Shilovskikh OS, Krzhizhanovskaya VV MG (2020c) Negevite, the pyrite-type  $\text{NiP}_2$ , a new terrestrial phosphide. *Am Mineral* 105:422–427
- Britvin SN, Krzhizhanovskaya MG, Zolotarev AA, Gorelova LA, Obolonskaya EV, Vlasenko NS, Shilovskikh VV, Murashko MN (2021a) Crystal chemistry of schreibersite,  $(\text{Fe,Ni})_3\text{P}$ . *Am Mineral* 106:1520–1529
- Britvin SN, Murashko MN, Vapnik Ye, Vlasenko NS, Krzhizhanovskaya MG, Vereshchagin OS, Bocharov VN, Lozhkin MS (2021b) Cyclophosphates, a new class of native phosphorus compounds, and some insights into prebiotic phosphorylation on early Earth. *Geology* 49:382–386
- Britvin SN, Vereshchagin OS, Shilovskikh VV, Krzhizhanovskaya MG, Gorelova LA, Vlasenko NS, Pakhomova AS, Zaitsev AN, Zolotarev AA, Bykov M, Lozhkin MS, Nestola F (2021c) Discovery of terrestrial allabogdanite  $(\text{Fe,Ni})_2\text{P}$ , and the effect of Ni and Mo substitution on the barringerite-allabogdanite high-pressure transition. *Am Mineral* 106:944–952
- Britvin SN, Murashko MN, Krzhizhanovskaya MG, Vereshchagin OS, Vapnik Ye, Shilovskikh VV, Lozhkin MS, Obolonskaya EV (2022a) Nazarovite,  $\text{Ni}_{12}\text{P}_5$ , a new terrestrial and meteoritic mineral structurally related to nickelposphide,  $\text{Ni}_3\text{P}$ . *Am Mineral*. doi: <https://doi.org/10.2138/am-2022-8219>
- Britvin SN, Murashko MN, Vereshchagin OS, Vapnik Ye, Shilovskikh VV, Vlasenko NS, Permyakov VV (2022b) Expanding the speciation of terrestrial molybdenum: discovery of polekhovskiyite,  $\text{MoNiP}_2$ , and insights into the sources of Mo-phosphides in the Dead Sea Transform area. *Am Mineral*. doi: <https://doi.org/10.2138/am-2022-8261>
- Britvin SN, Vlasenko NS, Aslandukov A, Aslandukova A, Dubrovinsky L, Gorelova LA, Krzhizhanovskaya MG, Vereshchagin OS, Bocharov VN, Shelukhina YuS, Lozhkin MS, Zaitsev AN, Nestola F (2022c) Natural cubic perovskite,  $\text{Ca}(\text{Ti,Si,Cr})\text{O}_{3-\delta}$ , a versatile potential host for rock-forming and less common elements up to Earth's mantle pressure. *Am Mineral*. doi: <https://doi.org/10.2138/am-2022-8186>
- Bruker (2004) SAINT-Plus and XPREP. Bruker AXS Inc., Madison, Wisconsin, USA
- Bruker (2005) APEX2. Bruker AXS Inc., Madison, Wisconsin, USA
- Burg A, Starinsky A, Bartov Y, Kolodny Y (1992) Geology of the Hatrurim Formation (“Mottled Zone”) in the Hatrurim basin. *Isr J Earth Sci* 40:107–124
- Burisch M, Gerdes A, Walter BF, Neumann U, Fettel M, Markl G (2017) Methane and the origin of five-element veins: mineralogy, age, fluid inclusion chemistry and ore forming processes in the Odenwald, SW Germany. *Ore Geol Rev* 81:42–61
- Buseck PR (1969) Phosphide from meteorites: barringerite, a new iron–nickel mineral. *Science* 165:169–171
- Chen K, Jin Z, Peng Z (1983) The discovery of iron barringerite,  $(\text{Fe}_2\text{P})$ , in China. *Sci Geol Sin* 1983:199–202
- Dera P, Lavina B, Borkowski LA, Prakapenka VB, Sutton SR, Rivers ML, Downs RT, Boctor NZ, Prewitt CT (2008) High-pressure polymorphism of  $\text{Fe}_2\text{P}$  and its implications for meteorites and Earth's core. *Geophys Res Lett* 35:L10301
- Dera P, Lavina B, Borkowski LA, Prakapenka VB, Sutton SR, Rivers ML, Downs RT, Prewitt CT (2009) Structure and behavior of the barringerite Ni end-member,  $\text{Ni}_2\text{P}$ , at deep Earth conditions and implications for natural Fe–Ni phosphides in planetary cores. *J Geophys Res Solid Earth* 2009:114
- Dolomanov OV, Bourhis LJ, Gildea RJ, Howard JA, Puschmann H (2009) OLEX2: a complete structure solution, refinement and analysis program. *J Appl Cryst* 42:339–341
- Eremenko GK, Polkanov YuA, Gevork'yan VKh (1974) Cosmogenic minerals in Paltava deposits of Konka-Yalynskoy depression in North-Azov region. *Mineralogiya Osadochnikh Obrazovaniy* 1:66–76 (in Russian)
- Essene EJ, Fisher DC (1986) Lightning strike fusion- extreme reduction and metal-silicate liquid immiscibility. *Science* 234:189–193
- Fleurance S, Cuney M, Malartre M, Reyx J (2013) Origin of the extreme polymetallic enrichment (Cd, Cr, Mo, Ni, U, V, Zn) of the Late Cretaceous–Early Tertiary Belqa Group, central Jordan. *Palaeogeogr Palaeoclimatol Palaeoecol* 369:201–219
- Geller YI, Burg A, Halicz L, Kolodny Y (2012) System closure during the combustion metamorphic “Mottled Zone” event, Israel. *Chem Geol* 334:25–36
- Gilat A (1994) Tectonic and associated mineralization activity, Southern Judea, Israel. *Geol Surv Isr Rep GSI/19/94*, Jerusalem, 322 p
- Grapes R (2011) *Pyrometamorphism*. Springer-Verlag, Berlin Heidelberg, p 365
- Gross S (1977) The mineralogy of the Hatrurim Formation, Israel. *Bull Geol Surv Israel* 70:1–80
- Guérin R, Sergent M, Chaudron G (1975) Synthèse et étude radiocristallographique des systèmes MP–MoP et MP–WP (M = élément 3d). *Compt Rend Acad Sci C* 281:777–780
- Guérin R, Sergent M (1977) Nouveaux arseniures et phosphures ternaires de molybdène ou de tungstène et d'éléments 3d, de formule:  $\text{M}_2-x\text{Me}_x\text{X}$  (M = élément 3d; Me = Mo, P) *Mater Res Bull* 12:381–388 W; X = As
- Ifandi E, Zaccarini F, Tsikouras B, Grammatikopoulos T, Garuti G, Karipi S, Hatzipanagiotou K (2018) First occurrences of Ni–V–Co phosphides in chromitite of Agios Stefanos mine, Othrys ophiolite. *Greece Ophiolite* 43:131–145
- Issar A, Eckstein Y, Bogoch R (1969) A possible thermal spring deposit in the Arad area, Israel. *Isr J Earth Sci* 18:17–20
- Ivanov AV, Zolensky ME, Saito A, Ohsumi K, MacPherson GJ, Yang SV, Kononkova NN, Mikouchi T (2000) Florenskiyite,  $\text{FeTiP}$ , a new phosphide from the Kaidun meteorite. *Am Mineral* 85:1082–1086
- Khoury HN, Salameh EM, Clark ID (2014) Mineralogy and origin of surficial uranium deposits hosted in travertine and calcrete from central Jordan. *Appl Geochem* 43:49–65
- Kolodny Y, Burg A, Geller YI, Halicz L, Zakon Y (2014) Veins in the combusted metamorphic rocks, Israel; weathering or a retrograde event? *Chem Geol* 385:140–155
- Kumar S, Krishnamurthy A, Bipin K, Srivastava K, Daa A, Paranjpe S (2004) Magnetization and neutron diffraction studies on  $\text{FeCrP}$ . *Pramana* 63:199–205
- Leblanc M (1986) Co–Ni arsenide deposits, with accessory gold, in ultramafic rocks from Morocco. *Can J Earth Sci* 23:1592–1602
- Litasov KD, Bekker TB, Sagatov NE, Gavryushkin PN, Krinitsyn PG, Kuper KE (2020)  $(\text{Fe,Ni})_2\text{P}$  allabogdanite can be an ambient pressure phase in iron meteorites. *Sci Rep* 10:8956
- Ma C, Beckett JR, Rossman GR (2014) Monipite,  $\text{MoNiP}$ , a new phosphide mineral in a Ca–Al-rich inclusion from the Allende meteorite. *Am Mineral* 99:198–205
- Martin L, Leemann L, Milodowski A, Mader U, Münch B, Giroud N (2016) A natural cement analogue study to understand the long-term behaviour of cements in nuclear waste repositories: Maqarin (Jordan). *Appl Geochem* 71:20–34
- Martin-Crespo T, Vindel E, Lopez-Garcia JA, Cardellach E (2004) As–(Ag) sulphide veins in the Spanish Central System: further evidence for a hydrothermal event of Permian age. *Ore Geol Rev* 25:199–219
- Minyuk PS, Plyashkevich AA, Subbotnikova TV, Al'shevskiy AV (2014) The magnetism of mineral phases of the Kolyma fulgurite. In «The paleomagnetism and magnetism of rocks», Proc Intern School–Seminar 7–12 Oct 2013, Kazan State Univ, Kazan, Russia, 156–162 (in Russian)

- Murashko MN, Vapnik Y, Polekhovskiy YP, Shilovskikh VV, Zaitsev AN, Vereshchagin OS, Britvin SN (2019) Nickolayite, IMA 2018 – 126. *Mineral Mag* 83:143–147 CNMNC Newsletter No. 47, February 2019, page 146
- Miyawaki R, Hatert F, Pasero M, Mills SJ (2019) IMA 16-F: Changes to CNMNC procedures regarding combustion products forming on burning coal dumps. *CNMNC Newsl* No 50; *Mineral Mag* 83:619
- Nishanbaev TP, Rochev AV, Kotlyarov VA (2002) Iron phosphides from the burned coal dumps of Chelyabinsk coal basin. *Uralsky Geol J* 25(1):105–114 (Russian)
- Novikov I, Vapnik Ye, Safonova I (2013) Mud volcano origin of the Mottled Zone, Southern Levant. *Geosci Front* 4:597–619
- Oliyynyk AO, Lomnytska YF, Dzevenko MV, Stoyko SS, Mar A (2013) Phase Equilibria in the Mo-Fe-P System at 800°C and Structure of Ternary Phosphide ( $\text{Mo}_{1-x}\text{Fe}_x$ ) $_3\text{P}$  ( $0.10 \leq x \leq 0.15$ ). *Inorg Chem* 52:983–991
- Orishchin SV, Kuz'ma YuB (1982) Interaction between the components in the ternary system W-Co-P. *Soviet Powder Metall Metal Ceram* 21(5):395–397
- Orishchin SV, Babizhetskii VS, Kuz'ma YuB (1998) Preparation and Structure of  $\text{Re}_3\text{P}_4$  Crystals. *Inorg Mater* 34(12):1227–1230
- Orishchin SV, Babizhetskii VS, Kuz'ma YuB (2000) Reinvestigation of the  $\text{NiP}_2$  structure. *Crystallogr Rep* 45(6):894–895
- Orishchin SV, Zhak OV, Budnik SL, Kuz'ma YuB (2002) The Y-Fe-P system. *Zhurn Neorg Khim* 47(9):1541–1545
- Pasek MA, Block K, Pasek V (2012) Fulgurite morphology: a classification scheme and clues to formation. *Contrib Mineral Petrol* 164:477–492
- Pauly H (1969) White cast iron with cohenite, schreibersite and sulphides from Tertiary basalts on Disko, Greenland. *Medd Dansk Geol For* 19:8–26
- Pedersen AK (1981) Armalcolite-bearing Fe-Ti oxide assemblages in graphite-equilibrated salic volcanic rocks with native iron from Disko, Central West Greenland. *Contrib Mineral Petrol* 77:307–324
- Peretyazhko IS, Savina EA, Khromova EA (2021) Low-pressure (> 4 MPa) and high-temperature (> 1250°C) incongruent melting of marly limestone: formation of carbonate melt and melilite–nepheline paralava in the Khamaryn–Khural–Khiid combustion metamorphic complex, East Mongolia. *Contrib Mineral Petrol* 176:38
- Plyashkevich AA, Minyuk PS, Subbotnikova TV, Alshevsky AV (2016) Newly Formed Minerals of the Fe-P-S System in Kolyma Fulgurite. *Dokl Russ Acad Sci Earth Sci* 467:380–383
- Rundqvist S, Nawapong PC (1966) The crystal structure of  $\text{ZrFeP}$  and related compounds. *Acta Chem Scand* 20:2250–2254
- Savina EA, Peretyazhko IS, Khromova EA, Glushkova VE (2020) Melted rocks (clinkers and paralavas) of Khamaryn-Khural-Khiid combustion metamorphic complex in Eastern Mongolia: mineralogy, geochemistry and genesis. *Petrology* 28(5):431–457
- Sheldrick GM (2015) Crystal structure refinement with SHELXL. *Acta Crystallogr C* 71:3–8
- Sideridis A, Zaccarini F, Grammatikopoulos T, Tsitsanis P, Tsikouras B, Pushkarev E, Garuti G, Hatzipanagioutou K (2018) First occurrences of Ni-phosphides in chromitites from the ophiolite complexes of Alapaevsk, Russia and Gerakini Ormylia, Greece. *Ofioliti* 43:75–84
- Stoe (2003) WinXPow, v. 2.08. STOE & Cie GmbH, Darmstadt
- Vapnik Ye, Sharygin V, Sokol E, Shagam R (2007) Paralavas in a combustion metamorphic complex, Hatrurim Basin, Israel. *GSA Reviews in Engineering Geology* XVIII:133–153
- Vereshchagin OS, Pankin DV, Smirnov MB, Vlasenko NS, Shilovskikh VV, Britvin SN (2021) Raman spectroscopy: A promising tool for the characterization of transition metal phosphides. *J Alloys Compd* 853:156468
- Wilson AJC (1992) *International Tables for Crystallography: Mathematical, Physical, and Chemical Tables*; International Union of Crystallography, vol 3. Chester, UK
- Xiong F, Xu X, Mugnaioli E, Gemmi M, Wirth R, Grew ES, Robinson PT, Yang J (2020a) Two new minerals, badengzhuite,  $\text{TiP}$ , and zhiqinite,  $\text{TiSi}_2$ , from the Cr-11 chromitite orebody, Luobusa ophiolite, Tibet, China: Is this evidence for super-reduced mantle-derived fluids? *Eur J Mineral* 32:557–574
- Yang JS, Bai WJ, Rong H, Zhang ZM, Xu ZQ, Fang QS, Yang BG, Li TF, Ren YF, Chen SY, Hu J-Z, Su JF, Mao HK (2005) Discovery of  $\text{Fe}_2\text{P}$  alloy in garnet peridotite from the Chinese Continental Scientific Drilling Project (CCSD) main hole. *Acta Petrol Sin* 21:271–276
- Zaccarini F, Pushkarev E, Garuti G, Kazakov I (2016) Platinum-group minerals and other accessory phases in chromite deposits of the Alapaevsk ophiolite, Central Urals, Russia. *Minerals* 6:108
- Zaccarini F, Bindi L, Ifandi E, Grammatikopoulos T, Stanley C, Garuti G, Mauro D (2019a) Tsikourasite,  $\text{Mo}_3\text{Ni}_2\text{P}_{1+x}$  ( $x < 0.25$ ), a new phosphide from the chromitite of the Othrys ophiolite. *Greece Minerals* 9:248
- Zaccarini F, Ifandi E, Tsikouras B, Grammatikopoulos T, Garuti G, Mauro D, Bindi L, Stanley C (2019b) Occurrences of new phosphides and sulfide of Ni, Co, V, and Mo from chromitite of the Othrys ophiolite complex (Central Greece). *Per Ital Mineral* 2019:88
- Zolensky ME, Gounelle M, Mikouchi T, Ohsumi K, Le L, Hagiya K, Tachikawa O (2008) Andreyivanovite: a second new phosphide from the Kaidun meteorite. *Am Mineral* 93:1295–1299

**Publisher's Note** Springer Nature remains neutral with regard to jurisdictional claims in published maps and institutional affiliations.